The role of microstructure during fatigue crack growth in poly(aryl ether ether ketone) (PEEK)

K. S. Saib, W. J. Evans* and D. H. Isaac†
*Department of Materials Engineering and *IRC in Materials for High Performance Applications, Department of Materials Engineering, University of Wales Swansea, Swansea SA2 8PP, UK*
(Received 4 August 1992; revised 21 December 1992)

The fatigue crack growth performance of injection moulded poly(aryl ether ether ketone) (PEEK) has been characterized using standard compact tension specimens and computer controlled photomicroscopy for crack length measurement. The influence of the materials parameters molecular weight and degree of crystallinity have been assessed together with experimental variables such as loading waveform shape and specimen orientation. Plots of crack growth rate against stress intensity factor range have been constructed from the experimental measurements. A quantitative measure of degree of crystallinity was obtained for each material using wide-angle X-ray diffraction. Post-fracture investigations using scanning electron microscopy were carried out to elucidate fatigue crack growth mechanisms. The results indicated that waveform shape had no effect on fatigue crack growth response. No anisotropic behaviour was evident, but an increase in molecular weight significantly improved the resistance of PEEK to fatigue crack growth. Similarly, increased crystallinity enhanced fatigue performance to a small extent. It is suggested that cyclic modes dominate fatigue crack growth at low rates of crack growth. However, with increasing speed, static processes begin to interact with cyclic mechanisms. At the onset of instability, failure is essentially dominated by static fracture modes.

(Keywords: fatigue; fracture; PEEK; microstructure; crack growth)

INTRODUCTION

ICI began commercial production of poly(aryl ether ether ketone) (PEEK) in 1978. This was in response to the demand for easily processed thermoplastic polymers which matched the strength and stiffness of thermosets and were able to provide improved temperature capability and chemical resistance compared with current thermoplastics[1].

PEEK is a semicrystalline thermoplastic with a glass transition temperature (T_g) of 143°C and a melting temperature (T_m) of 334°C[2]. In comparison with aliphatic polymers, the presence in the backbone of phenyl groups restricts molecular chain mobility. Unlike other aromatic polymers, PEEK also contains ketone chain links. These are more rigid than ether linkages thus helping to raise both T_g and T_m[3]. Their rigidity is also responsible for the high strength and stiffness of PEEK and for the maintenance of these properties at useful levels up to relatively high temperatures (heat distortion temperature = 160°C). Since PEEK has a significantly lower density than metals or alloys it displays an excellent range of specific mechanical properties.

However, chain rigidity does tend to hinder the packing of molecules and limits the ultimate degree of crystallinity attainable. In commercial PEEK, crystallinity is normally in the range 25–35%. Even so, this semicrystalline nature is sufficient to provide PEEK with excellent chemical and hydrolysis resistance under both hot and high pressure conditions[4].

As a consequence of its excellent property portfolio, PEEK is available in a variety of forms: unreinforced, short and continuous fibre reinforced. It is developing into one of the most versatile of modern materials[5] and increasingly is being considered by designers for high stress bearing applications. In many of these design studies, resistance to fatigue is a crucial requirement. Characterization of fatigue crack development, therefore, is an essential prerequisite for PEEK-based materials to be used reliably, safely and efficiently in service applications.

It is perhaps surprising that the fatigue behaviour of unreinforced PEEK has received little attention. Usually, these basic fatigue properties are presented simply as a datum against which composites derived from PEEK can be compared[6]. The majority of research on unreinforced PEEK has focused on crystallization kinetics and microstructure (primarily degree of crystallinity and spherulite size) and their effects on monotonic mechanical properties[7,8].

Traditionally, fatigue capability has been presented in the form of stress amplitude against cycles to failure (or S/N) graphs. This representation can overestimate performance since the presence of inherent defects is not taken into consideration. Defects reduce or even eliminate the crack initiation stage of fatigue. Thus in

†To whom correspondence should be addressed

0032-3861/93/153198-06

situations where defects or stress concentrations are known to be present, it has become more usual to base estimates of component lifetimes on crack growth response through the application of fracture mechanics principles. This approach relies on a detailed quantitative characterization of crack growth behaviour. Furthermore, fractographic information gathered from fatigue crack growth tests can contribute to the development of models describing the mechanisms and kinetics of crack growth in these novel materials. Such analyses also allow the application of defect tolerant design methodologies.

This paper reports fatigue crack growth results for two grades of unreinforced PEEK. The information presented is extracted from a wider study of fatigue in a range of short glass and carbon fibre reinforced PEEK composites[9–13]. Particular attention here is given to macroscopic fatigue behaviour and to possible micromechanisms of crack growth. The roles of molecular weight, degree of crystallinity, anisotropy and load waveform are assessed.

EXPERIMENTAL

Materials

Two grades of injection moulded unreinforced PEEK were supplied by ICI (*Table 1*). These were experimental materials based on commercially available 450G (high molecular weight) and 150G (low molecular weight) Victrex PEEK. The two grades are known to have similar static properties but the lower molecular weight version has superior mould filling properties as a result of its lower melt viscosity. Mouldings were in the form of 3 mm thick edge coat-hanger gated plaques. This mould geometry has the advantage of a relatively uniform microstructure in both planar and through thickness directions.

In order to assess the influence of degree of crystallinity on fatigue performance, the 450G material was post-annealed (denoted by the suffix, PA) at 320°C for 1 h followed by furnace cooling[14]. The aim of this treatment was to maximize the degree of crystallinity and hence, clarify the roles that crystallinity and molecular weight play in fatigue failure. During heat treatment, the plaques were sandwiched between two heavy flat metal sheets to prevent warping.

Table 1 Material descriptions and degrees of crystallinity from WAXD

Material	Description	X_c (%)
150G	Low molecular weight PEEK	29
450G	High molecular weight PEEK	28
450G, PA	Post-annealed high molecular weight PEEK	34

Crystallinity

The degree of crystallinity for each unreinforced grade was defined quantitatively by means of wide-angle X-ray diffraction (WAXD). Transmission WAXD photographs were obtained using a Philips PW1720 generator and a universal flat plate PW1030 camera. Throughout, Ni-filtered CuKα X-radiation was employed. The X-ray photographs were sent to the SERC Daresbury Laboratory for digitization using a Joyce-Loebl SCANDIG-3 microdensitometer. This digitized information was stored on magnetic tape for subsequent processing into linear intensity scans from which it was possible to calculate the degree of crystallinity[15]:

$$X_c = \frac{I_c}{I_c + I_a} \quad (1)$$

where I_c is the area bounded by the linear intensity scan of crystalline scatter and I_a is the area bounded by the linear intensity scan of amorphous scatter. Background air scatter was accounted for by obtaining a diffraction pattern in the absence of a polymer sample. The area bounded by this linear intensity scan was subtracted in each case.

Specimens

The compact tension (CT) geometry shown in *Figure 1* was chosen in preference to alternatives. It has been widely used in fatigue crack growth and fracture toughness studies on polymers and short fibre composites. The CT geometry has a predominantly bend stress state which permits smaller sizes for plane strain conditions at the crack tip than other configurations[16]. This is an advantage because injection moulded articles (such as plaques) normally have relatively small thicknesses and planar dimensions. Crack initiation is straightforward in the CT geometry and the subsequent crack growth is stable over a wide range of crack sizes[17]. For the fatigue crack growth data to be valid (i.e. geometry independent), specimen thickness must be large enough to ensure plane strain conditions at the crack tip and the planar dimensions must be such as to preclude buckling. The specimen thickness was determined by the constraints of

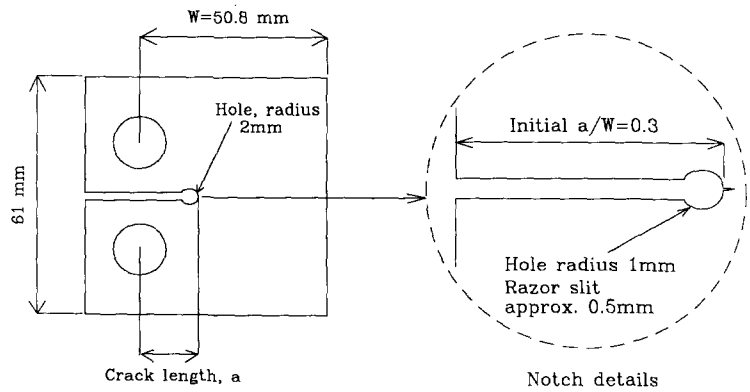

Figure 1 Compact tension specimen geometry with notch details employed for fatigue crack growth testing

the injection moulding technique. The specimen planar dimensions were consistent with conditions specified in ASTM E647[18].

The inset in *Figure 1* illustrates the notch details. It was essentially a slot ending in a drilled hole ASTM E399[19] as specified in the American standards for plane strain fracture toughness determination. This configuration was chosen for its ease of manufacture. A drilling jig was used to produce the holes for the loading pins and for shaping the notch tip radius. It ensured that the loading geometry was symmetrical and virtually identical in all specimens. To facilitate initiation of a through thickness crack, a razor blade was used to introduce a 'starter slit' at the root of the machined radius. To achieve some level of reproducibility in starter slit length, the specimen was held in an Instron wedge action grip. The razor blade was then depressed into the material at the root of the notch to a nominal depth of 0.5 mm, using a position control ramp.

All specimens were machined directly from the moulded plaques. Notches were always cut from the edge of the plaque towards the centre. To aid optical crack length measurement, the specimen was vacuum sputter coated with aluminium prior to testing. In order to study the effects of anisotropy, specimens were cut both parallel and perpendicular to the mould filling direction (MFD). These were defined as 0° (loading parallel to the MFD) and 90° (loading perpendicular to the MFD) specimens, respectively.

Crack growth testing

The crack growth tests were carried out in load control using an Instron 1341 servohydraulic testing machine. For comparison with work carried out by Jones *et al.*[5], a square wave load cycle with a stress ratio, R (minimum stress/maximum stress), of 0.1 was adopted. A limited number of tests on 450G(0°) were conducted using a sine waveform for comparison purposes. A cyclic frequency of 1 Hz was used to minimize heating effects. Temperature monitoring confirmed rises of <15°C above ambient. All fatigue testing was carried out in an air conditioned laboratory (18°C). Control and data acquisition were via an Apricot microcomputer and CIL intelligent interface. Crack lengths were measured by computed controlled photomicroscopy. The system automatically controlled intervals between photographs by monitoring the crack opening displacement of the CT specimen. Testing was carried out until normalized crack lengths $\alpha = a/W$ of ~ 0.4–0.45 had been attained, where a is the crack length and W is the width of the CT specimen. Beyond this, the speed of crack growth was too high to allow accurate crack length measurement.

Crack length (a) was measured as a function of the number of cycles (N). These data were used to determine the crack growth rate (da/dN) at the ith cycle as a function of stress intensity factor range (ΔK) using the methods described in ASTM E647[18]:

$$(da/dN)_{a_i} = \frac{a_{i+1} - a_{i-1}}{N_{i+1} - N_{i-1}} \quad (2)$$

$$\Delta K = \frac{\Delta P}{B\sqrt{W}} \frac{(2+\alpha)}{(1-\alpha)^{1.5}} \times (0.886 + 4.64\alpha - 13.32\alpha^2 + 14.72\alpha^3 - 5.6\alpha^4) \quad (3)$$

where ΔP is the load range applied and B is the sample thickness. The reduced data were plotted on a log–log basis.

Microscopy

Fracture surfaces were analysed using a Jeol 35C scanning electron microscope. Samples were cut to size and mounted on steel stubs using a solution of colloidal silver in acetone and then vacuum sputter coated with a thin layer of gold. Fractographs were taken for each material in regions of similar fatigue stressing history (typically where $\Delta K \approx 4.5$ MPa $m^{1/2}$). Additionally, characteristic features in regions of static fracture (i.e. catastrophic failure at the end of a fatigue crack growth test) were recorded.

RESULTS

Fatigue crack growth

Crack growth data in the form of crack length (a) as a function of the number of cycles elapsed (N) are plotted in *Figure 2*. This figure contains crack growth curves for 450G(0°) cycled at different nominal stress ranges. It is clear that the rate at which the cracks propagate is strongly dependent on stress range.

The crack growth rates (da/dN) derived from these curves are plotted against ΔK on a log–log basis in *Figure 3*. The graph clearly displays the three regions frequently associated with fatigue crack growth. Below $\Delta K \approx 3$ MPa $m^{1/2}$, da/dN drops to vanishingly low levels and an apparent threshold condition is reached at $\Delta K \approx 2.5$ MPa $m^{1/2}$. In the intermediate region for $3 < \Delta K < 4.5$ MPa $m^{1/2}$ approximately, the data are consistent with a Paris law linear relationship[20]:

$$da/dN = A\,\Delta K^m \quad (4)$$

where A and m are constants for specific material and experimental conditions. Best fit lines, 99% tolerance bands and values of the constants A and m were obtained by a least squares regression analysis of the data in this region[9]. It was found that $A = 21.1 \times 10^{13}$ and $m = 6.37$ for as-received 450G(0°). Above $\Delta K \approx 4.5$ MPa $m^{1/2}$, the crack grows more rapidly than predicted by the Paris law as instability approaches.

The effect of loading waveform shape on fatigue crack growth in neat 450G(0°) is shown in *Figure 4*. A square

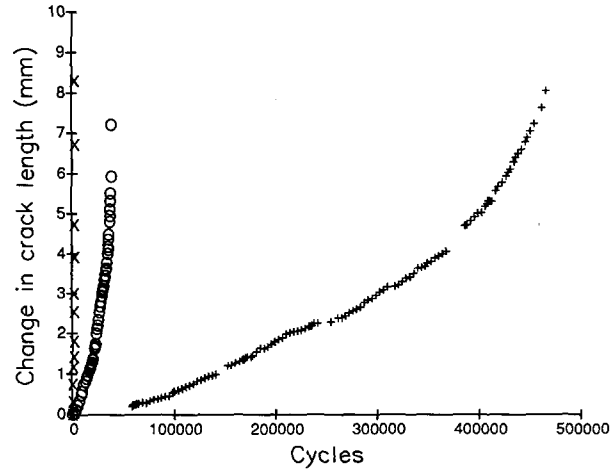

Figure 2 Fatigue crack growth curves for 450G(0°) at different nominal stress range levels: (+) 2.5 MPa; (○) 3.7 MPa; (×) 4.7 MPa

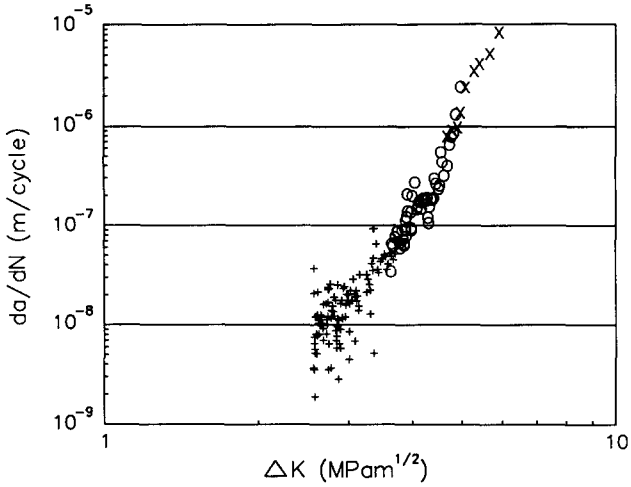

Figure 3 Fatigue crack growth behaviour in 450G(0°) at different nominal stress range levels: (+) 2.5 MPa; (○) 3.7 MPa; (×) 4.7 MPa

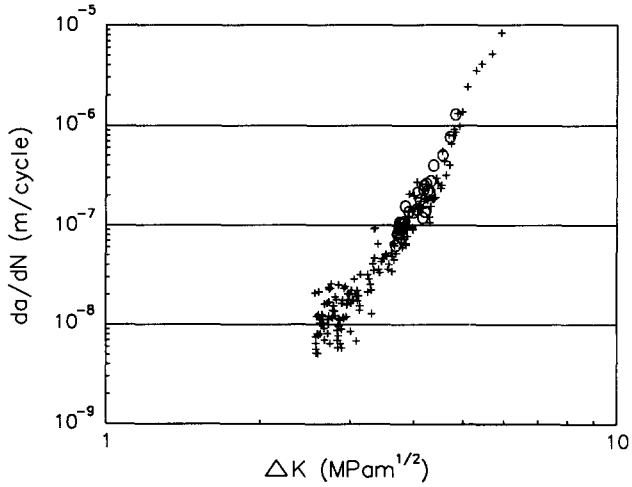

Figure 4 Effect of loading waveform shape on fatigue crack growth in 450G(0°): (+) square; (○) sine

waveform incorporates a dwell period at maximum load during which creep/static effects could interact with cyclic mechanisms. However, it is clear from *Figure 4* that crack growth rate data generated using a sine waveform accurately superimpose on data obtained with the square wave.

The effect of specimen orientation on fatigue crack growth in the 450G polymer is shown in *Figure 5*. There is no discernible anisotropy between 0° and 90° orientations for neat 450G. In *Figure 6*, the role of molecular weight is assessed. It is apparent that the as-received 450G matrix exhibits superior fatigue crack growth behaviour to the lower molecular weight 150G. The 150G material develops growth rates that are almost an order of magnitude higher for the same ΔK.

Annealing raised the degree of crystallinity (X_c) of 450G PEEK (*Table 1*). The effects of this annealing treatment on fatigue crack growth are shown for the 450G material in *Figure 7*. The increase in crystallinity appears to have produced a small improvement in fatigue crack growth resistance. Thus, whereas as-received 450G displays accelerated growth rates at $\Delta K > \sim 4.5$ MPa m$^{1/2}$, the effect of annealing is to extend the Paris law region to higher ΔK values. Hence the post-annealed data lie on an extension of the best fit Paris law line for the as-received 450G(0°).

Fractography

Figures 8–10 are a selection of micrographs, obtained from CT specimens fractured in fatigue. They illustrate typical features associated with the range of materials studied at $\Delta K \approx 4.5$ MPa m$^{1/2}$. For comparison, *Figure 11* shows the result of monotonic fracture of a CT

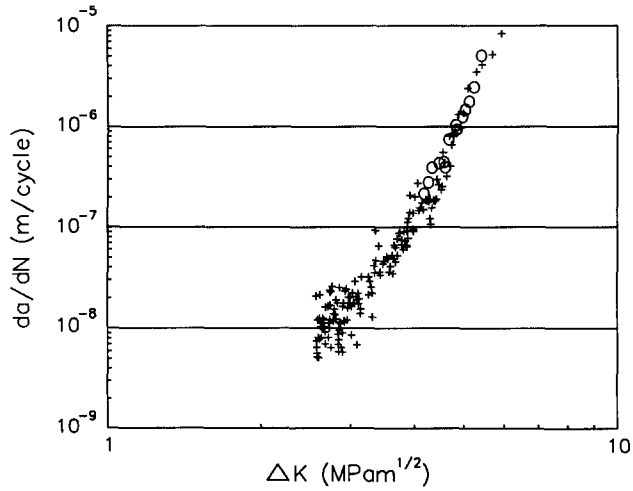

Figure 5 Effect of specimen orientation on fatigue crack growth in 450G: (+) 0°; (○) 90°

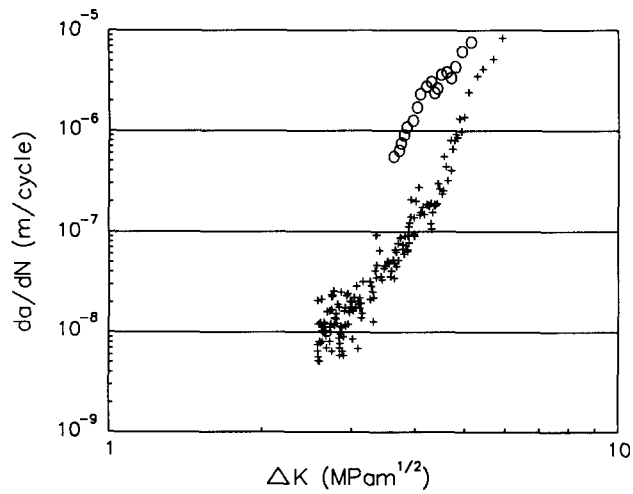

Figure 6 Effect of molecular weight on fatigue crack growth in PEEK (0°): (+) 450G; (○) 150G

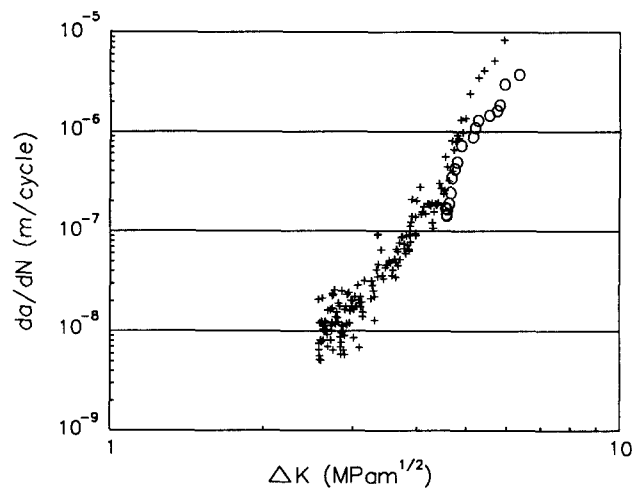

Figure 7 Effect of increased degree of crystallinity on fatigue crack growth in 450G(0°): (+) as-received; (○) post-annealed

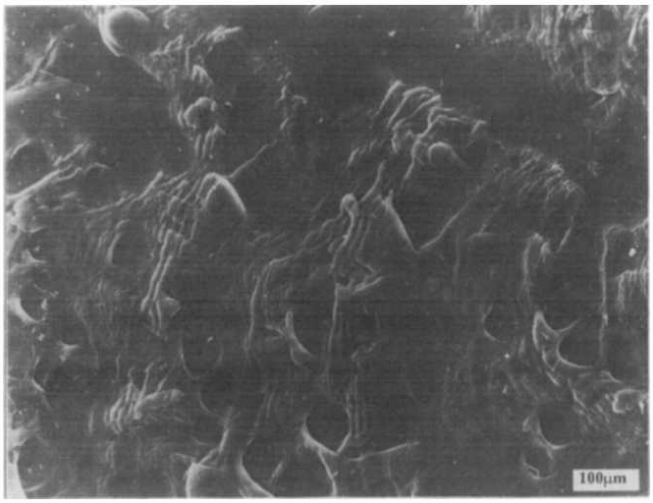

Figure 8 Fatigue crack growth fracture surface of as-received 450G(0°) at $\Delta K \approx 4.5$ MPa $m^{1/2}$

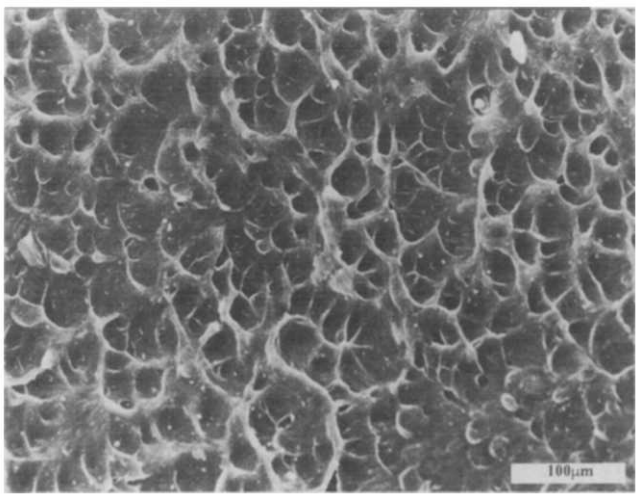

Figure 9 Fatigue crack growth fracture surface of as-received 150G(0°) at $\Delta K \approx 4.5$ MPa $m^{1/2}$

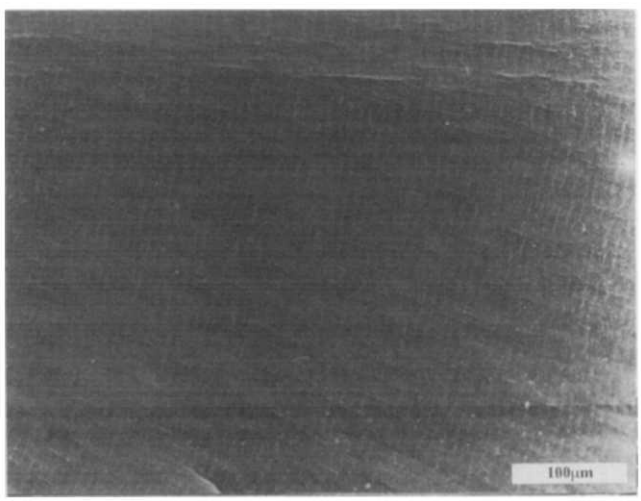

Figure 10 Fatigue crack growth fracture surface of post-annealed 450G(0°) at $\Delta K \approx 4.5$ MPa $m^{1/2}$

specimen. The crack growth direction was from left to right on each photograph.

In *Figure 8*, the surface of 450G(0°) is relatively flat, although parabolic regions of microductility are present. These are often surrounded by striation-like markings. A similar morphology is seen in the fracture surface of unreinforced 150G(0°) although no striation markings are evident (*Figure 9*). The effects of post-annealing 450G(0°) can be seen in *Figure 10* which has a flatter surface with a clear striation morphology. By measuring the average width of each band (a direct measure of da/dN), it was possible to confirm these markings as true fatigue striations by comparison with the Paris plot in *Figure 7*.

DISCUSSION

Micromechanical fatigue damage in unreinforced PEEK

With some polymers, discontinuous growth bands (DGBs) are seen on the fatigue fracture surface[21]. They are similar to fatigue striations in appearance but there is not a direct correspondence between the bands and the loading cycles. In this study, DGBs were not found on the fracture surfaces. During stable fatigue crack growth, true fatigue striations as shown in *Figure 10* occur. Since each striation is associated with one loading cycle, their width increases with crack growth rate.

Parabolic or dimpled regions similar to those in *Figures 8* and *9* have been noted previously for PEEK under monotonic loading[22]. They are considered to be formed by the intersection of the crack front with secondary cracks nucleated ahead in the plastic zone. As crack growth rate increases, the size of these microductile regions rises correspondingly. For comparison, *Figure 11* illustrates the fracture surface of a statically fractured sample of 450G(0°). It exhibits large parabolic regions confirming that these are characteristic of static failure processes.

On the basis of these observations, it would appear that crack growth in unreinforced PEEK at low rates of growth is essentially a cyclic phenomenon as emphasized by the presence of striations. However, as the rate increases, monotonic fracture mechanisms (dimples) begin to interact with the cyclic mode. Eventually, in the later stages of fatigue crack growth, the monotonic processes dominate.

This progression can be seen by comparing the growth rate plots in *Figures 5*, *6* and *7* and the fractographs in *Figures 8–10*. Post-annealed 450G(0°) is marginally superior in terms of fatigue crack growth resistance to

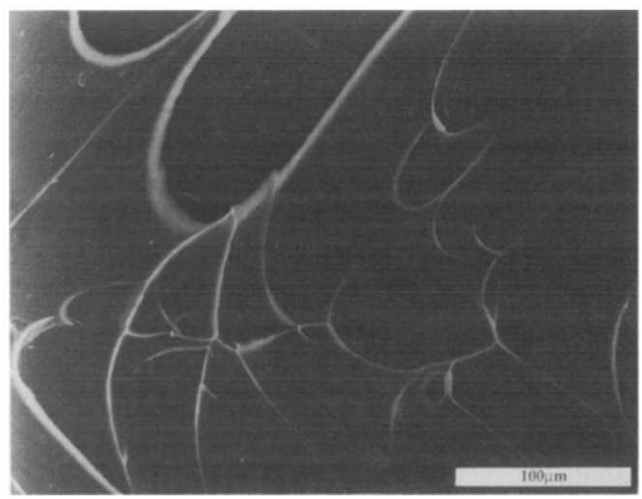

Figure 11 Monotonic fracture surface of as-received 450G(0°)

as-received 450G(0°) which is itself superior to 150G(0°). Hence, at $\Delta K \approx 4.5$ MPa $m^{1/2}$, each material is at a different stage of the fatigue crack growth process. The as-received 450G(0°) material (*Figure 8*) is at the transition point between cyclic and static mode dominated crack growth. Hence, both dimples and packets of striations are evident. However, a dominant monotonic mode of failure is clear for the least fatigue resistant material 150G(0°) since the fracture surface in *Figure 9* is almost entirely composed of dimples. This is consistent with the data of *Figure 6* which indicate that at $\Delta K \approx 4.5$ MPa $m^{1/2}$ the crack growth rate is beyond the Paris law region and accelerating. On the other hand, *Figure 10* shows that at this stress intensity factor level post-annealed 450G(0°) exhibits a classic fatigue striation morphology and no dimples are present. The annealing treatment has led to an extension of the stable Paris crack growth region of the as-received material (*Figure 7*). Thus the influence of static failure processes has been diminished at this level of ΔK presumably due to the increased level of crystallinity. At the same time, it would appear that the basic cyclic mode of crack growth is not affected by the change in crystallinity.

Microstructural parameters

Previous studies[23] have shown that in addition to molecular weight (MW) and crystallinity (X_c), a third parameter that can influence the mechanical properties of a thermoplastic is the tie molecule density, t. Tie molecules are chains which connect two or more lamellar crystals and as such exercise some control over the rigidity of the polymer. Runt and Jacq[24] have shown that an increase in either X_c or t improves resistance to fatigue crack growth. However, the situation is complicated further since the three variables themselves (MW, X_c and t) are interdependent. For example, an increase in MW for constant X_c results in an increase in t, whereas an increase in X_c for constant MW decreases t (refs 23, 24).

Although the two unreinforced materials had different molecular weights, their degrees of crystallinity were similar, implying a higher value of t in 450G. It is evident that this is associated with an improved resistance to crack growth, particularly at higher crack growth rates (*Figure 6*). The fractographs for 450G (*Figure 8*) and 150G (*Figure 9*) suggest that static failure modes may play a significant role in this regime, particularly for 150G. This would imply that tie molecules are significant in the development of static fracture processes.

In contrast, an increase in crystallinity from 28 to 34% appears to delay the onset of static failure (*Figure 7*). At lower growth rates, both as-received and post-annealed materials behave in a similar manner. At high growth rates, post-annealed 450G displays improved fatigue crack resistance and this is confirmed by the predominance of striations associated with cyclic fracture modes and the lack of static dimples in *Figure 10*. The increase in crystallite size and degree of order after annealing undoubtedly results in more energy being required to deform and fracture PEEK. Hence, the progress of a fatigue crack is hindered. It is also reasonable to assume that a post-annealing treatment is unlikely to change t dramatically and as such t does not play an important role in this instance where molecular weight is unchanged.

CONCLUSIONS

The PEEK materials studied have been found to obey the Paris law over a wide range of ΔK. No discernible effect of loading waveform shape or anisotropy was observed in the fatigue crack growth data for the 450G polymer. For these unreinforced samples, an increase in molecular weight resulted in significantly improved performance, since the onset of static failure processes was delayed by the presence of more tie molecules. A similar, though smaller, improvement was observed after post-annealing of 450G polymer, in this case as a consequence of the increased crystallinity since t is unlikely to be affected dramatically. It is suggested that t is a more significant parameter than the degree of crystallinity in delaying the onset of static damage. At low crack growth rates, fatigue crack growth in PEEK is dominated by cyclic mechanisms involving striation formation. As crack speed increases, parabolic regions of ductility associated with static processes interact with the cyclic modes of failure. As the fatigue crack approaches instability, static mechanisms dominate the failure process.

ACKNOWLEDGEMENTS

The authors would like to thank Dr D. R. Moore of ICI, Wilton Research Centre for valuable discussions throughout the work. KSS is grateful to the Victrex Group at ICI Materials for the supply of all materials and funding for a research studentship.

REFERENCES

1 Smith, C. P. *Swiss Plastics* 1981, **3**, no. 4
2 ICI Technical Data Sheet no. VK2/0586, 1986
3 Dawson, P. C. and Blundell, D. J. *Polymer* 1980, **21**, 577
4 ICI Technical Data Sheet no. VK1/1285, 1985
5 Jones, D. P., Leach, D. C. and Moore, D. R. *Polymer* 1985, **26**, 1385
6 Friedrich, K., Walter, R., Voss, H. and Karger-Kocsis, J. *Composites* 1986, **17**, 205
7 Cebe, P. *J. Mater. Sci.* 1988, **23**, 3721
8 Seferis, J. C. *Polym. Comp.* 1986, **7**, 158
9 Saib, K. S. *PhD Thesis* University of Wales, 1991
10 Saib, K. S., Evans, W. J. and Isaac, D. H. 'Proc. Joint FEFG/ICF Int. Conf. on Fracture of Engineering Materials and Structures', Singapore, Elsevier, London, 1991, pp. 215–220
11 Saib, K. S., Evans, W. J., and Isaac, D. H. 'Proc. 1st Int. Conf. on Deformation and Fracture of Composites', UMIST, Plastics and Rubber Institute, London, 1991, pp. 9/1–9/6
12 Saib, K. S., Evans, W. J. and Isaac, D. H. 'Processing and Manufacturing of Composite Materials', ASME, Atlanta (PED, Vol. 49; MD, Vol. 27), ASME, New York, 1991, pp. 261–275
13 Saib, K. S., Evans, W. J. and Isaac, D. H. 'Proc. 20th Bi. Conf. on Carbon', University of California at Santa Barbara, American Carbon Society, Santa Barbara, 1991, pp. 272–273
14 Chivers, R. A. and Moore, D. R. *Polymer* in press
15 Campbell, D. and White, J. R. 'Polymer Characterisation – Physical Techniques', Chapman and Hall, London, 1989
16 Williams, J. G. Testing Protocol-EGF Task Group on Polymers and Composites, 1988
17 Kinloch, A. J. and Young, R. J. 'Fracture Behaviour of Polymers', Applied Science Publishers, London, 1983
18 ASTM E647-81, Annual Book of ASTM Standards, 1981, Pt 10
19 ASTM E399-81, Annual Book of ASTM Standards, 1981, Pt 10
20 Karger-Kocsis, J. in 'Applications of Fracture Mechanics to Composite Materials' (Ed. K. Friedrich), Elsevier, London, 1989, pp. 189–247
21 Hertzberg, R. W. and Manson, J. A. 'Fatigue of Engineering Plastics', Academic Press, New York, 1980
22 Chu, J.-N. and Schultz, J. M. *J. Mater. Sci.* 1989, **24**, 4538
23 Greco, R. and Ragosta, G. J. *J. Mater. Sci.* 1988, **23**, 4171
24 Runt, J. and Jacq, M. *J. Mater. Sci.* 1989, **24**, 1421